Computational Simulation and Comparison of the Effect of Different Surroundings on Wind Loads on Domed Structures

Jin-Shian Lin[1], Cheng-Hsin Chang[2] and Neng-Chou Shang[3]

[1]*Department of Water Resources and Environmental Engineering, Tamking University, Tamsui, Taiwan 251, R.O.C.*
[2]*Department of Civil Engineering, Tamking University, Tamsui, Taiwan 251, R.O.C.*
[3]*Graduate Institute of Environmental Engineering, National Taiwan University, Taipei, Taiwan 106, R.O.C.*

Abstract

Mean surface pressures and overall wind loads on domes immersed in a boundary layer were obtained by computational fluid dynamics simulation. The effects of alternative turbulence models, upwind area roughness were examined and compared with wind tunnel studies. Surface pressures on dome structures were calculated in two cases by numerical simulation. One is with surrounding structures to calculate the wind comes from east and west direction, another one is no surrounding structure existing. The results will be evaluated the accuracy of numerical simulation with different roughness types of upwind area and effect of surroundings. Calculated values were compared to wind-tunnel measurements made in equivalent flow conditions.

Key Words: Wind Load, Wind Engineering, Computational Fluid Dynamics, Dome Structure

1. Introduction

Domes are commonly used to enclosed large spaces due to the structural efficiency and consequent economic benefit. These structures are sensitive to load distributions and they are excellent at resisting symmetric loading. Although domes are excellent at resisting symmetric loading, the structures are sensitive to asymmetric loading that may cause failure or loss of cladding. Many wind tunnel studies have been undertaken to determine wind loads on domes and hemispheres in boundary layer flows. Early work by Maher [1] was in uniform flow with little approach flow turbulence. Other authors included a turbulent shear flow over a range of Reynolds numbers. Taniguchi & Sakamato [2], 1981; Toy et al., 1983 [3]; Newman et al., [4]; Savoy & Toy, [5], but only Ogawa et al. [6], Taylor [7] and Letchford and Sarkar [8] presented measurements of fluctuating pressures. Letchford and Sarkar provided dual dome mean, rms and peak pressure contours and loads. Recently, many studies focus on the computation fluid dynamics simulation of the wind load on doom structures. Meroney [9] compared the numerical and wind tunnel simulation of mean pressure distributions over single and paired dome sets. Horr, et al. [10] used the CFD analysis to create a computational wind tunnel to derive the pressure loading on large domes. Chang and Meroney [11] also examined the effect of surroundings with different separation distances on surface pressures on low-rise buildings in both wind tunnel and CFD models.

This study uses Computational Fluid Dynamic (CFD) methods to examine mean Cp on surface of domes in different type of up-wind areas and to compare the effects of turbulent model selected with previous wind-tunnel studies. The results of comparison shows accuracy not only in turbulent model selected, but also in different roughness type of up-wind areas in the same numerical setup. For example, Figure 1 shows that there is no structure and building located in area of west side of domes (west is coast), but a lots of surrounding buildings and structures in east side. The approaching wind direction which comes from

*Corresponding author. E-mail:cc527330@mail.tku.edu.tw

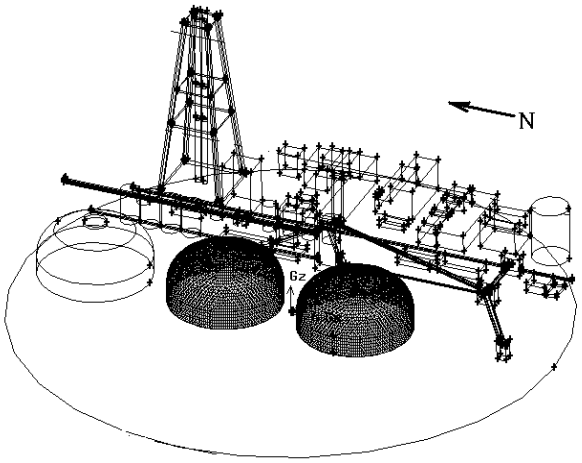

Figure 1. Configuration of dooms and surrounding area.

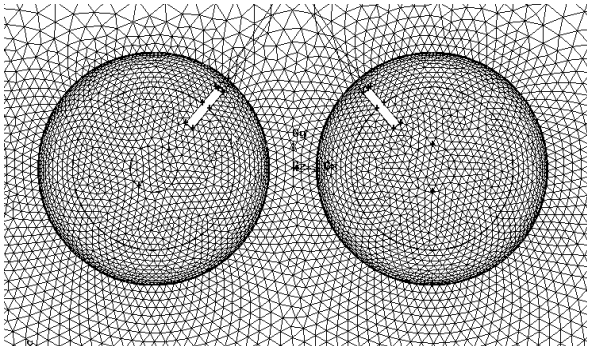

Figure 2. Unstructured mesh used tetrahedral mesh generation.

west or east gets the totally different type of surrounding pattern in the up wind area. One is nothing located in the front of the doom. Another is surroundings located in the front of it. A commercial code suite FLUENT 6.0 and Gambit 2.1 produced by FLUENT© Inc. were used to perform the calculations rather than codes created to be application specific to determine whether software in the public domain would suffice to produce results suitable for design purposes. Figure 2 is the example shows the unstructured grid mesh around the doom area.

2. Dome Geometry and Wind Tunnel Configuration

A wind-tunnel study of coal storage domes [12], to be located at the Hsinta indoor coal yard of the Taiwan Power Company near Kaohsiung, Taiwan, was conducted to determine wind load on the surface of doom. Aluminum models of the complex of four domes were fabricated to a 1:200 scale and centered on a turntable in the wind tunnel. One of the domes was instrumented with 260 pressure taps to measure exterior pressures exerted by the wind. Figure 3a shows the geometry of the doom and the locations of pressure tap (black dots). Replicas of surrounding structures within a 285-m radius (or more for certain azimuths) were constructed and placed on the turntable. The instrumented model was tested in two alternate positions, and symmetry was further utilized to obtain peak local maximum and minimum pressures applicable to all of the domes.

The wind-tunnel testing was performed in the natural boundary-layer wind tunnel of Cermak Peterka Petersen, Inc., Fort Collins, Colorado. The wind-tunnel test was

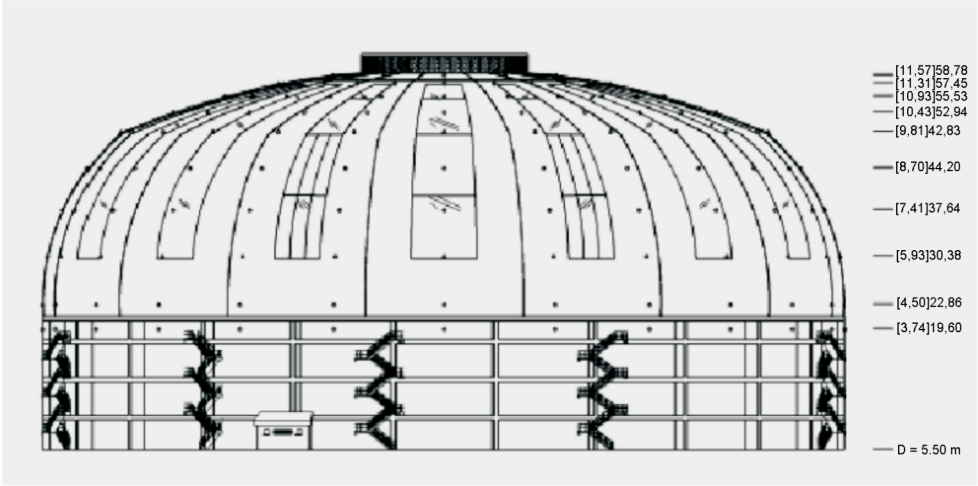

Figure 3a. Details of the instrumented model with locations of pressure tap.

performed in the closed-circuit boundary-layer wind tunnel. This wind tunnel has a 20.6-m-long test section covered with roughness elements to reproduce at model scale the atmospheric wind characteristics required for the model test. The wind tunnel has a flexible roof, adjustable in height, to maintain a zero pressure gradient along the test section and to minimize blockage effects. Other buildings or terrain features located nearby can have an important influence on wind loads. Consequently, the surrounding area was modeled in detail to a radius of 285 m using styrofoam and wood. The dome model and surrounding structures are mounted on the turntable located near the downstream end of the wind-tunnel test section. Figure 3b shows the picture of wind tunnel setup.

An approach boundary layer representative of an open-country environment was established in the test section of the wind tunnel. The boundary layer had a mean wind speed profile power-law exponent of 0.14 and the mean velocity and turbulence intensity at model apex height were 18 m/s and 15%, respectively. Test Reynolds Number was approximately $4.8*10^5$. These boundary layer characteristics were also the target values for inlet conditions to the test domain for the numerical calculations.

Measurements of external pressures were made for each pressure tap location for 36 wind directions. Pressures at all locations were measured five times to decrease experimental uncertainty via the mechanism of ensemble averaging.

All pressures were non-dimensionalized into pressure coefficients by dividing by the mean dynamic pressure at the top of the dome [i.e. $Cp =)p/(\frac{1}{2}\rho U^2)$]. Dynamic pressure behavior was also measured during the wind-tunnel tests, but such data cannot be calculated by conventional numerical procedures from the Reynolds averaged Navier Stokes equations. Alternative nonsteady numerical techniques using time dependent calculations, direct numerical simulation, or large-eddy turbulence models can reproduce such information, but were not used in this comparison study.

Figure 3b. Photographs of the completed model in wind tunnel.

3. Numerical Procedure

The numerical simulation tool used in this study was computational fluid dynamics, commercial code, Fluent. The Fluent CFD software was based on a finite volume discretization of the equations of motion, an unstructured grid volume made of either rectangular prisms or tetrahedral cells, various matrix inverting routines, and, in this case, either kappa-epsilon (κ-ε) or renormalized group theory kappa-epsilon (RNG-κ-ε) turbulence models. Steady state solutions were sought for several flow configurations, and the data generated were displayed on various isopleth contour plots of velocity, pressure, and turbulence. Particle trajectories were also generated to elucidate the effects of dome spacing. The code was run on a Pentium 4 2.4 GHz PC using a Microsoft XP operating system with 1 GB Memory Ram. Most of the previous studies of numerical simulation of windload were concerned on only different sharps of building without surrounding building since limitations of computing capabilities. In this study not only doom structures included calculating domain, but also complicate surrounding included.

3.1 Inlet Conditions to the Numerical Domain

The wind tunnel inlet flow of velocity and turbulence intensity can be used for calculating CFD inlet flow boundary conditions. The wind tunnel data and input profiles of velocity, turbulent kinetic energy, and dissipation used for the numerical simulation are shown on Figure 4. The inlet values of kinetic energy, *k,* and dissipation ratio, ε, are calculated from measured velocity profiles and turbulence intensities with a given friction velocity ratio, u_*/u_{ref} for the wind tunnel setup, according to Equation (1) and Equation (2).

Where, *y* is distance from the wall, κ is the von Karman constant.

$$k = \frac{3}{2}\sqrt{u^{'2}} \tag{1}$$

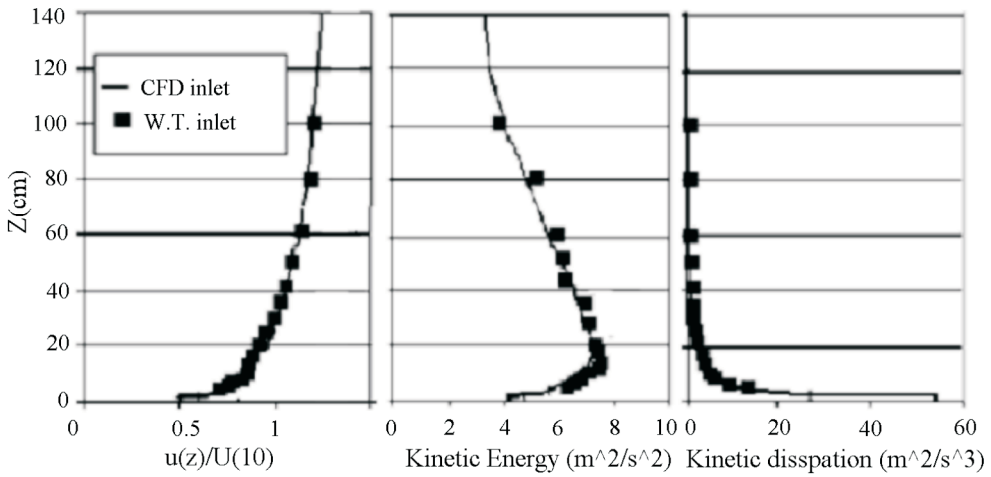

Figure 4. Numerical inlet velocity and kinetic energy profile compared to approach velocity profile.

$$\varepsilon = \frac{u_*^3}{\kappa y} \tag{2}$$

All velocity profiles are collinear, and the numerical and wind tunnel kinetic energy and dissipation ratio are very similar as well.

3.2 Numerical Domain and Meshes

Version 6.0 of the FLUENT code was used for all numerical simulations. Inlet profiles were prepared by spreadsheet and save as inlet boundary condition file. The inlet mean velocity, turbulent kinetic energy and dissipation profiles were similar to those measured in the wind tunnel and in dynamic equilibrium with one another. The ground surface roughness measured during the laboratory experiments was $1.4*10^{-4}$ m or an equivalent sand roughness, k, equal to 4 mm. Values deduced from the numerical wind tunnel for these parameters were $1.7*10^{-4}$ m and 5 mm, respectively. All velocity profiles are essentially collinear, and the numerical and wind tunnel turbulence intensity values are also very similar.

Three calculation domains were chosen, depending on with or without surrounding structures and the approaching wind orientation. The typical numerical domain represented a 3 m wide wind tunnel, 2 m flow depth, and a 5 m test section length. The example of three domes configuration without surrounding (case 1) shown in Figure 5 contained some 452,730 cells, 947,167 faces and 97,124 nodes distributed over 12 face zones. The example of three domes configuration with surrounding structures (Caes 2 and 3) shown in Figure 6 contained some 709,911 cells, 1,483,114 faces and 149,971 nodes dis-

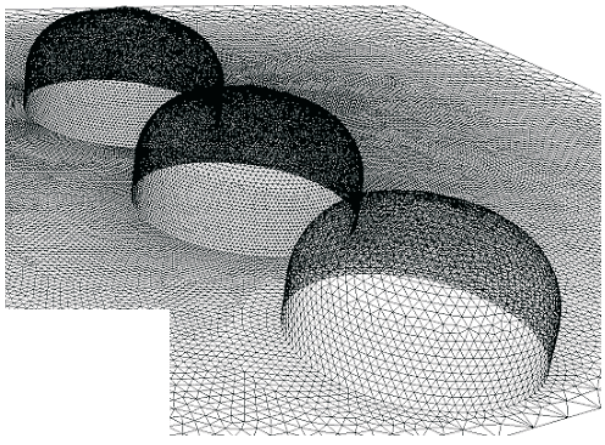

Figure 5. Configuration of dooms without surroundings.

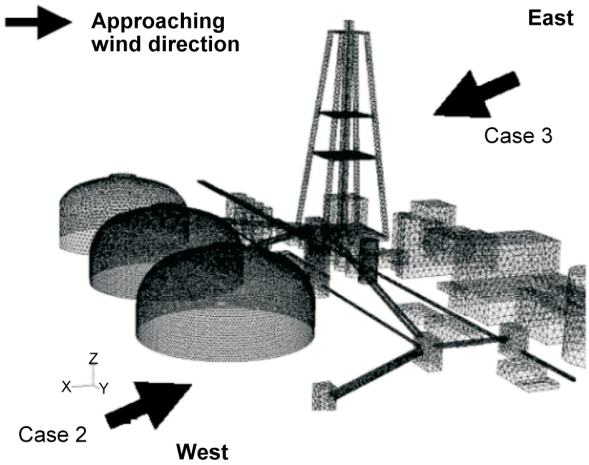

Figure 6. Configuration of dooms with surroundings.

tributed over 12 face zones. Outlet and velocity inlet or symmetry boundaries were specified at the sides and top of the grid volume, while appropriate surface roughness was specified at the ground. The inflow boundary conditions were chosen to match the velocity and turbulence profiles measured during the wind-tunnel experiments. Outflow boundary conditions were chosen to maintain constant longitudinal rate of change of all dependent variables.

4. Results and Comprasion

4.1 Wind Tunnel Result

Since the doom structures are symmetric, the different approaching wind directions do not affect the loading behavior on the structures. Only different wind speeds and profiles can get the different results of load behavior. Flow approaching the single dome decelerates along the centerline, stagnates against the surface and produces a maximum mean pressure coefficient stagnation region of about Cp = -0.5~-0.7 at a height of y/h = 0.3 for all of three numerical cases. An extremely weak horseshoe shaped vortex forms on the front face and wraps around the dome downwind. The flow accelerates over the cupola of dome producing a minimum mean pressure coefficient region of about Cp = -1~-1.3 that lies across the cupola roof of the dome. The flow decelerates again as it descends over the back of the dome, and the pressure coefficient decreases gradually over the very end of the dome down to the ground. The wind tunnel simulations of case 2 and case 3 are the examples of with and without surroundings which caused the change on approaching wind profiles due to the shielding effects. Figure 7 shows the centerline mean pressure coefficient profiles over the dooms of case 2 and case 3. The maximum mean pressure coefficient are found at locations of a height of y/h = 0.3 on the downwind wall and around -0.7 and -0.55 for case 2 and case 3. Comparison results show that case 3 has lower Cp values due to the shielding effects.

Figure 8 compares the mean centerline pressure coefficient distribution plotted versus projected stream wise direction on the central dome with that measured by CPP and numerical simulation using Fluent for Case 1 and Case 2 which the approaching wind comes form West direction. Both the numerical calculations and the Wind tunnel display positive pressure coefficients over the downwind face of the dome. Figure 9 makes the same comparison for the Case 3, approaching wind from East direction. Results of CFD show that two cases have the closed predicting accuracies and over prediction of mean Cp on the flow separation regions.

5. Conclusion

Mean pressure distributions over domes have been calculated for different upwind surrounding structures. The results show that numerical simulation by using Fluent commercial code software can predict the trend of mean pressure coefficient on the surface of doom, Even through the geometry of surrounding structures are very complicated. The only restricts are the capacity of the computer and simulation times.

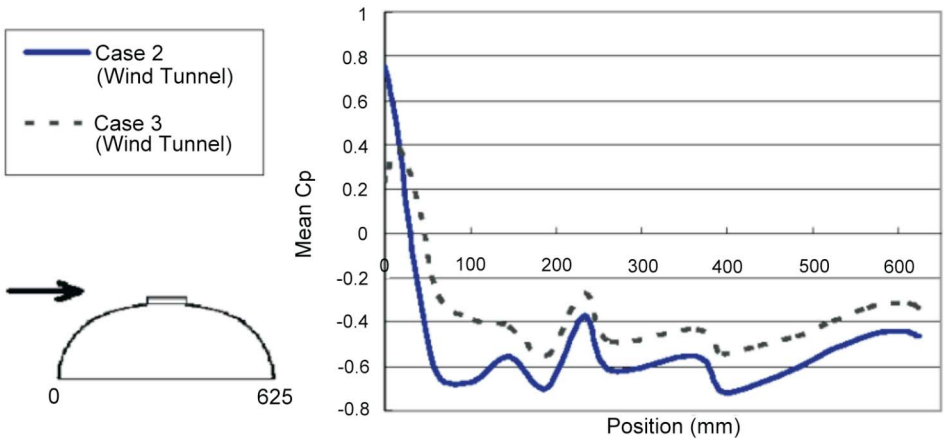

Figure 7. Centerline mean pressure coefficient profile for approaching wind directions of west and east.

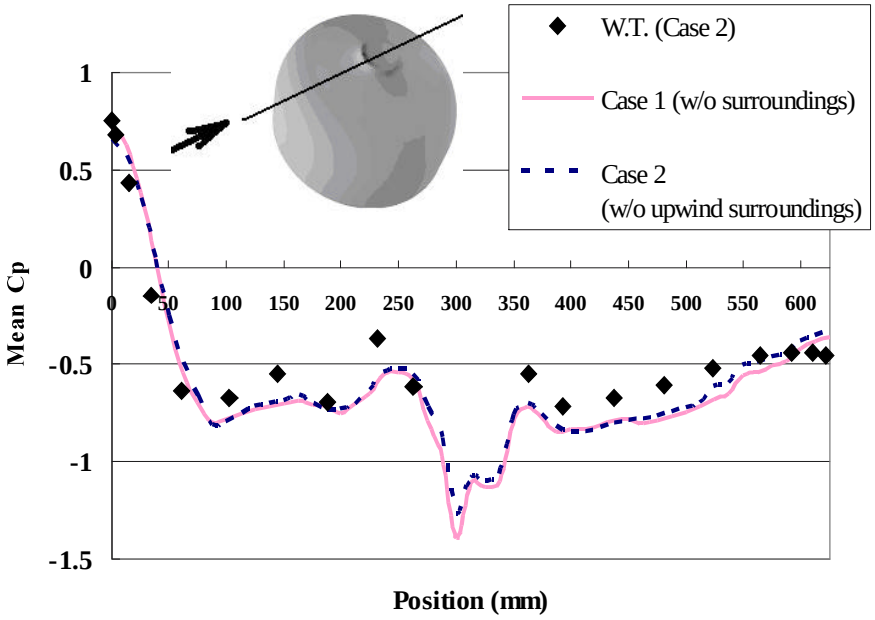

Figure 8. The comparison of mean centerline pressure coefficient distribution of wind tunnel data and numerical date (case 1 and 3).

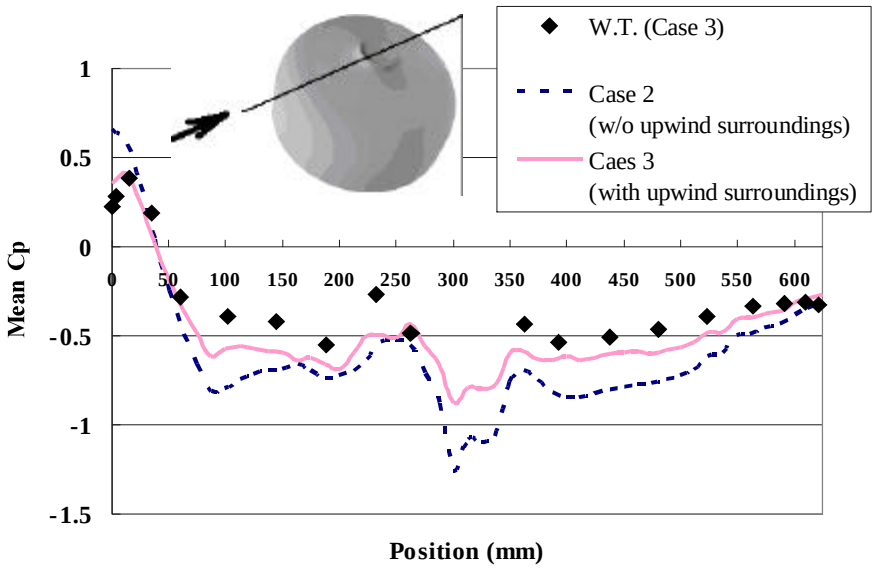

Figure 9. The comparison of mean centerline pressure coefficient distribution of wind tunnel data and numerical date (case 2 and 3).

References

[1] Cedric Price Architects, F., Newby, R. H. and Suan, J. S., Felix and Partners, "Air Structures: A Survey", Department of the Environment, London, HMSO, UK (1971).

[2] Bird, W. W., "Design Manual for Spherical Radomes (Revised), Cornell Aeronautical Laboratory, Report UB-909-D2 (1965).

[3] Toy, N., Moss, W. D. and Savory, E., "Wind Tunnel Studies on a Dome in Turbulent Boundary Layers", *Journal of Wind Engineering and Industrial Aerodynamics*, Vol. 1, pp. 201–212 (1983).

[4] Newman, B. G., Ganguli, U. and Shristava, C., "Flow over Spherical Inflated Buildings," Journal *of Wind Engineering and Industrial Aerodynamics*, Vol. 17,

pp. 305–327 (1984).

[5] Savory, E. and Toy, N. "Hemispheres and Hemisphere-Cylinders in Turbulent Boundary Layers," *Journal of Wind Engineering and Industrial Aerodynamics,* Vol. 23, pp. 345–354, (1986).

[6] Ogawa, T., Nakayama, Murayama, S. and Sasaki, Y., "Characteristics of Wind Pressures on Basic Structures with Curved Surfaces and Their Response in Turbulent Flow," *Journal of Wind Engineering and Industrial Aerodynamics,* Vol. 38, pp. 427-438 (1991).

[7] Letchford, C. W. and Sarkar, P. P., "Mean and Fluctuating Wind Loads on Rough and Smooth Domes", *Proceedings of BBAA IV Colloquium,* Ruhr-Univ Bochum, Germany, pp. 19 (2000)

[8] Taylor, T. J., "Wind Pressures on a Hemispherical Dome," *Journal of Wind Engineering and Industrial Aerodynamics,* Vol. 40, pp. 199–213 (1991).

[9] Meroney, R. N., "Comparison of Numerical and Wind Tunnel Simulation of Wind Loads on Smooth, Rough and Dual Domes Immersed in a Boundary Layer," *Proceedings of CWE 2000* (2000).

[10] Horr, A. M., Safi, M. and Alavinasab, S. A., "Computational Wind Tunnel Analyses for Large Dome Using CFD Theory," *International Journal of Space Structures,* Vol. 18, pp. 85–104 (2003).

[11] Chang, C. H. and Meroney, R. N., "The Effect of Surroundings with Different Separation Distances on Surface Pressures on Low-Rise Buildings", *Journal of Wind Engineering and Industrial Aerodynamics,* Vol. 91, pp. 1039–1050 (2001).

[12] Boggs Daryl, W., "Final Report, Wind-Tunnel Tests — Coal Storage Domes Hsinta Indoor Coal Yard, Kaohsiung, Taiwan," Cermak Peterka Petersen, Inc., CPP Project 02-2397 (2002).

Manuscript Received: Jul. 26, 2004
Accepted: Dec. 8, 2005